

## GaAs 웨이퍼의 대역단 영상에 대한 정량적 해석

강성준\* · 나철훈

### Quantitative Analysis on Near Band Edge Images in GaAs Wafer

Seong-jun Kang\* · Cheolhun Na

Department of Electronics, Information and Communication Engineering, Mokpo National University, Muan 58554, Korea

#### 요 약

도핑 되지 않은 반 절연 LEC GaAs 내의 EL2와 얇은 준위 분포를 영상화하기 위해 대역단 적외선 영상 기법을 활용했다. 대역단 적외선 투사 매핑에 근거한 본 기법은 분석 속도가 빠르고 비파괴적인 방법이다. EL2 흡수 영상이 콘트라스트 반전되는 대역단 부근에 대한 정량적인 해석은 아직 보고되지 않고 있다. 본 논문은 대역단 부근에서 영상의 특정 부분(cell, wall)에 대한 포토퀀칭 메커니즘의 스펙트럼-, 공간- 및 온도- 종속성을 논하고 있다. 결함 부분별(EL2w, EL2b)로 포토퀀칭 개시점이 다른 것은 불순물 종류의 차이로 인한 서로 다른 전기적 작용에 기인한 것으로 해석할 수 있다. 전위(dislocation) 밀도가 높은 곳에서는 EL2b 밀도는 약간 적은 반면 EL2w 밀도는 보다 많다는 것을 정량적 해석으로부터 확인 했다.

#### ABSTRACT

Near band infrared imaging technique has adopted for imaging EL2 and shallow level distributions in undoped semi-insulating LEC GaAs. This technique, which relies on the mapping of near bandgap infrared transmission, is both rapid and non-destructive. Until now no quantitative analysis has been reported for near band edge region which gives the reverse contrast on EL2 absorption images. This paper presents the spectral, spatial and temperature dependence of photoquenching forward and inverse mechanism in the band edge domain for cells and walls and for direct and inverted contrast conditions during transitory regimes. The difference in the threshold for the EL2w and EL2b defects could be attributed to the contribution of a different electrical assistance due to a different species of impurities. Quantitative analysis results show an increased density of EL2w and a small reduction of EL2b in the region of the walls where there is a high density of dislocations.

**키워드** : 대역단, 스펙트럼 영상화, 반 절연 GaAs 웨이퍼, 콘트라스트 반전

**Key word** : Defect concentration, Spectral imaging, LEC grown SI GaAs, Near band edge

Received 29 December 2016, Revised 19 January 2017, Accepted 10 April 2017

\* Corresponding Author Seong-Jun Kang(E-mail: sjkang@mokpo.ac.kr, Tel:+82-61-450-2742)

Department of Electronics, Information and Communication Engineering, Mokpo National University, Muan 58554, Korea

Open Access <https://doi.org/10.6109/jkiice.2017.21.5.861>

print ISSN: 2234-4772 online ISSN: 2288-4165

©This is an Open Access article distributed under the terms of the Creative Commons Attribution Non-Commercial License(<http://creativecommons.org/licenses/by-nc/3.0/>) which permits unrestricted non-commercial use, distribution, and reproduction in any medium, provided the original work is properly cited.  
Copyright © The Korea Institute of Information and Communication Engineering.

## I. INTRODUCTION

LEC (liquid encapsulated Czochralski) grown semi-insulating (SI) Gallium Arsenide (GaAs) is an important material at the present time as a substrate for optoelectronic IC fabrication. One of the most important properties of the substrate is that it should be uniform over large areas. In order to investigate the uniformity of GaAs wafers several infrared imaging techniques have been developed [1, 2]. The observed infrared inhomogeneities have been attributed to fluctuations in the concentrations of the native defect, usually designated as EL2. The material is semi-insulating due to the presence of the deep donor EL2 which pins the Fermi level very close to the center of the GaAs bandgap. This EL2 defect was historically discovered amongst many other levels in photocapacitance spectroscopy experiments. It gained notoriety due to its unusual property to be transformed into a metastable and passive configuration after illumination by infrared light at low temperature: This is the photoquenching (PQ) phenomenon. i.e., At low temperature ( $T < 80$  K) the absorption in the high EL2 density regions is significantly decreased after white light illumination. This “bleaching” thermally recovers if the temperature is raised above 130 K.

Infrared transmission (IRT) images as well as scattering tomography (LST) provide an internal view of the crystal disorder [2]. Patterns are revealed which coincide with the arrangement of threaded dislocations; schematically “wall” are formed which limit the internal volume of defect free “cells”.

The PQ conversion of EL2 is seen as a bleaching of the pattern. This bleaching property allows us to monitor the EL2 which have been turned to metastable state. This differential evaluation is academically considered as the best solution for evaluating the EL2 density [2].

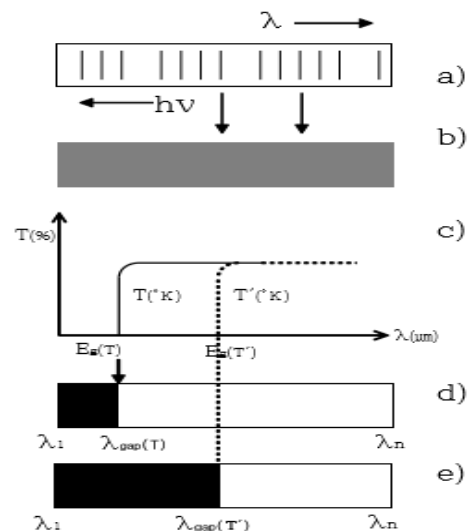
It has also been discovered that a contrast inverted pattern replaces the direct contrast image near band edge, especially after the PQ.

In this paper we present a study of the spectral, spatial

and temperature dependence of the PQ forward and inverse mechanism in the band edge domain for cells and walls.

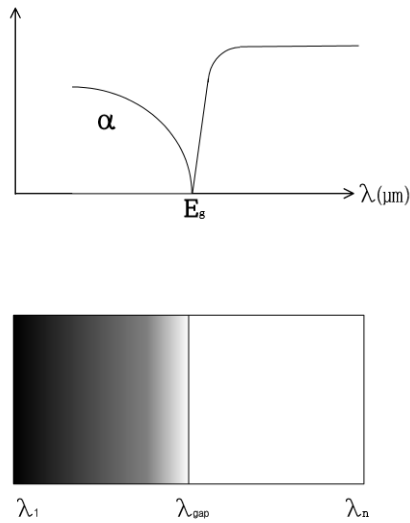
## II. SPECTRAL IMAGING

Fig.1 illustrates the near band spectral imaging principle used in the present paper. A light source, such as, infrared rays having a wavelength band of  $0.8\text{--}0.9\ \mu\text{m}$  around the energy gap, is irradiated onto a semiconductor sample [Fig. 1(a), (b)]. Fig. 1(c) shows the transmission spectrum of a semiconductor at different temperatures. The resulting spectral characteristic of the light band transmitted through the sample can be depicted as in Fig. 1(d), (e). By sliding the transmission spectrum of the Fig. 1(c) with varying the temperature, we can obtain temperature-dependent edges images like Fig. 1(d), (e). By applying a digital image processing algorithm to those images, we can analysis quantitatively the details in the near band regions



**Fig. 1** Diagrammatic construction of the principle employed in the present technique. (a)  $0.8\text{--}0.9\ \mu\text{m}$  band infrared rays, (b) sample, (c) transmission spectrum at different temperature ( $T$ : lower temp.,  $T'$ : higher temp.), (d,e) resultant images at different transmission spectra.

In reality, the absorption coefficient  $\alpha$  increases as photon energy increases Fig.2 (a), so the actual image will appear like the one in Fig. 2 (b). That is, as more light is absorbed, the more the image darkens. The  $\lambda_1$  side in Fig. 2(b) represents the lowest gray level.



**Fig. 2** Absorption/transmission spectrum of a sample and resultant image according to absorption coefficients.

The experimental set-up has been previously described [3], it consists of a cryostat containing the GaAs wafer and the cryostat is equipped with large glass windows. The circulating liquid Helium allows the sample to be cooled down to 10 K. Photoquenching was carried out using a tungsten halogen bulb to provide white light illumination of the sample: Several durations and intensities were tested in order to reach a saturated PQ effect. It was verified that selecting the observation wavelength at  $\lambda=1 \mu\text{m}$  using an interference filter does not introduce any changes in the images obtained before and after PQ. Also it was observed that selecting a wavelength in the high absorption gap region ( $\lambda = 0.85 \mu\text{m}$ ) leads to an inverted image of the cells after PQ.

The samples are from LEC grown undoped SI materials (Thomson, Cominco, thickness  $d = 350 \mu\text{m}$  and 5 mm).

### III. PRINCIPLES OF QUANTITATIVE ANALYSIS

The transmitted intensity  $I$  through an absorbing media, with allowance for multiple reflections at the parallel faces is

$$I = I_0 \frac{(1-R)^2 \exp(-\alpha d)}{1-R^2 \exp(-2\alpha d)} F_s \quad (1)$$

where  $R$  is the reflectivity,  $\alpha$  is the absorption coefficient,  $d$  the wafer thickness, and  $F_s$  describes the spatial variation of scattering processes. In GaAs the absorption coefficient can be separated into two parts, one due to EL2 and the other related to all other absorption processes:

$$\alpha = \alpha_{EL2} + \alpha_1 \quad (2)$$

This is the case for a normal GaAs wafer, but if EL2 is in its quenched state  $\alpha_{EL2} = 0$  and the absorption coefficient can be written as  $\alpha = \alpha_1$ .

The ratio between the transmitted intensity  $I$  and the transmitted intensity through the quenched wafer  $I_Q$  is

$$\begin{aligned} \frac{I}{I_Q} &= \frac{I_0 \frac{(1-R)^2 \exp[-(\alpha_1 + \alpha_{EL2})d]}{1-R^2 \exp[-2(\alpha_1 + \alpha_{EL2})d]} F_s}{I_0 \frac{(1-R)^2 \exp(-\alpha_1 d)}{1-R^2 \exp(-2\alpha_1 d)} F_s} \\ &= \exp(-\alpha_{EL2} d) \frac{1-R^2 \exp(-\alpha_1 d)}{1-R^2 \exp[-2(\alpha_1 + \alpha_{EL2})d]} \quad (3) \end{aligned}$$

Equation (3) is approximated by

$$\frac{I}{I_Q} = \exp(-\alpha_{EL2} d) \quad (4)$$

Equation (4) gives us an error of 10% compared with the full expression, but it does not rely on any assumptions for the reflections [4]. The absorption

coefficient,  $\alpha_{EL2}$ , is calculated as

$$\alpha_{EL2} = \frac{1}{d} \ln \left( \frac{I_Q}{I} \right) \quad (5)$$

From equation (5), an absolute value of the EL2 concentration is calculated as

$$N_{EL2} = \frac{\alpha_{EL2}}{\sigma_{EL2}} \quad (6)$$

where  $\sigma_{EL2}$  is the absorption cross-section of EL2. Therefore the concentration [EL2] is easily obtained if we know the optical cross-section of  $\sigma_{EL2}$ . As an example,  $\sigma_{EL2}$  can be obtained from literature for arbitrary photon energies [5].

#### IV. RESULTS AND DISCUSSION

The experimental procedure is as follows : Illumination is provided by a halogen lamp on the conventional infrared imaging setup described above. In order to obtain a spectral band covering the 0.8~0.9  $\mu\text{m}$  domain, a monochromator whose output slit being removed is placed at the back of halogen lamp. Polychromatic light passes through the sample, and the vidicon camera captures the resulting images. These images are displayed on the image monitor and stored on a image storage system.

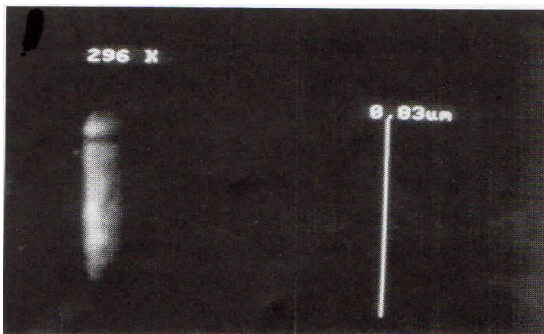
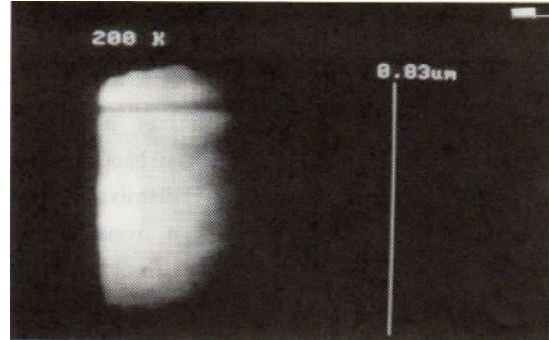
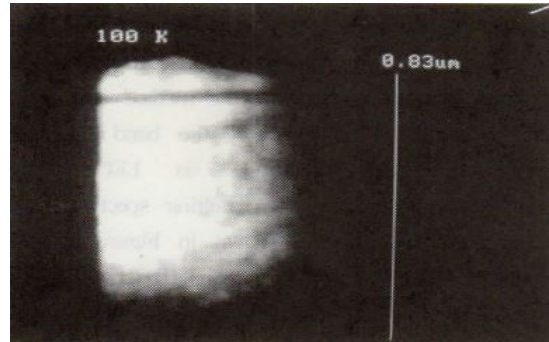


**Fig. 3** Spectral image of an undoped GaAs material at room temperature.



(a)



(b)



(c)

**Fig. 4** Spectral images at 200 K (a), 100 K (b) and 10 K (c) during thermal relaxation.

The resulting spectral image at room temperature is shown in Fig. 3. After changing the sample temperature, the above imaging process is repeated. Fig. 4 shows the images at different temperatures of 10 K, 100 K and 200 K respectively. These images are well agreed with the theory (described in Fig. 1).

The transmission images is observed with a uniform illumination at a wavelength of  $1 \mu\text{m}$  (positive contrast); This allowed us to select a place in the sample where a linear and uniform “streamer” was clearly observable as a dark line horizontally crossing the image field. This feature was used as a reference of the “wall” transmission with comparison to the neighboring clear background later referred to as “cell” transmission. Both cell and wall measurements are made along the x axis (i.e. wavelength) and lead to contrast calculation. During transmission observation it was verified that the illumination level is low enough not to perturb appreciably the PQ state. An example of these spectral images is given in Fig. 5 referring to the respective situations, before (a) and after (b) PQ at  $T = 10 \text{ K}$ . For the sake of photographic observability, these images were especially processed along vertical bands to extend the observation on the right hand side.

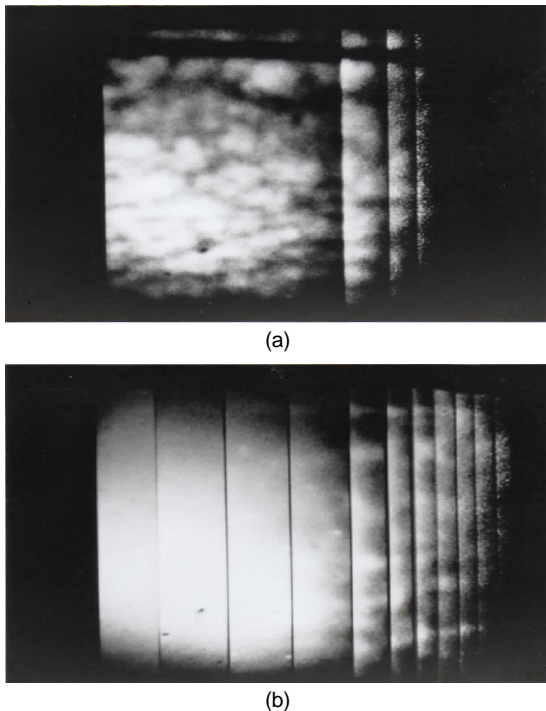


**Fig. 5** Spectral images before (a) and after (b) PQ at  $T=10 \text{ K}$ , positive and negative contrasts are respectively observed.

Direct observation in the spectral image of the PQ effect at  $10 \text{ K}$  clearly shows that:

i) in the  $1.2\text{-}0.9 \mu\text{m}$  range the contrast is strongly affected by PQ but a weak positive structure still remains which is ascribed to the residual scattering losses on the decoration precipitates.

ii) in the band edge region the contrast becomes negative after removing the EL2 absorption pattern. This region of inverse contrast extends over some  $80 - 100 \text{ meV}$  under the gap limit.

Three typical lines (A:  $0.858 \mu\text{m}$ , B:  $0.864 \mu\text{m}$ , C:  $0.875 \mu\text{m}$ , see Fig. 6) were selected (respectively 63, 76, 104 meV from the band edge at  $T=10 \text{ K}$ ).

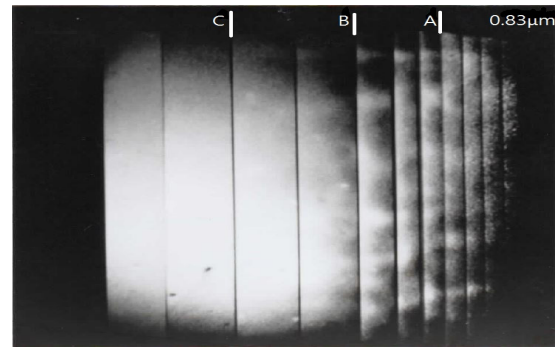


**Fig. 6** Reference image for the spectral lines A, B, C.

Clearly A belongs to the negative contrast zone, C to the positive one and B is the limit in between. It was verified that the C line is representative of the conventional EL2 behavior in agreement with Skolnick [1].

The cryostat was then allowed to warm up and the thermal relaxation was measured every  $10 \text{ K}$ : The raw data of pixel values before PQ at  $10 \text{ K}$  and at some typical temperatures during thermal relaxation after PQ are given in Table 1: Corresponding plots of the contrast evolution are given in Fig 7 for the lines A, B, C.

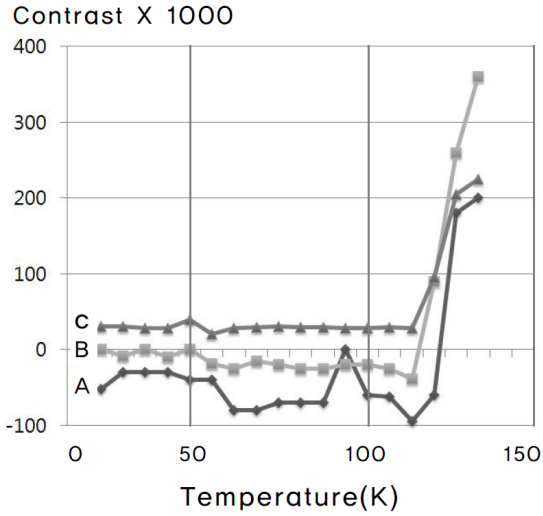


Fig. 7 Thermal recovery of optical transmission (cell) after 10 K PQ.

Table. 1 Raw data of gray levels for cell and wall as a function of temperatures. Relative contrast is defined as  $(I_c - I_w) / (I_c + I_w)$ .

Spect. line	A			B			C		
	C	W	Ctr	C	W	Ctr	C	W	Ctr
10 (before PQ)	39	17	+0.390	54	24	+0.380	62	31	+0.330
10 (after PQ)	80	90	-0.58	116	116	0.000	138	130	+0.029
20	84	90	-0.034	112	114	-0.080	138	128	+0.030
40	78	84	-0.037	16	108	-0.090	130	124	+0.023
60	70	78	-0.054	102	106	-0.019	132	128	+0.015
80	62	72	-0.075	98	102	-0.020	132	124	+0.031
100	54	62	-0.089	90	94	-0.022	128	122	+0.016
120	40	48	-0.090	74	80	-0.039	118	114	+0.017
125	28	32	-0.087	62	54	+0.069	98	82	+0.089
130	20	14	+0.170	42	24	+0.270	64	42	+0.207
135	12	8	+0.200	34	18	+0.360	54	34	+0.227

C : Cell( $I_C$ )    W : Wall( $I_W$ )    Ctr : Contrast

The transmission level identically recovers at  $T = 125$  K for the three lines, This observation means that the thermal recovery mechanism is the same for direct and reverse contrast spectral zones, which implies that the negative contrast contribution does not refer to a special EL2 mechanism. From this experiment it also follows that the fundamental optical absorption associated to the EL2 PQ transformation largely extends to the energy gap.

Another series of experiments was performed in which the PQ temperature was varied. As stated in reference [2], the background transmission starts increasing for a PQ temperature under 125 K whereas the image structure (contrast) vanishes only for PQ temperatures below some 70-80 K(Fig. 8). It follows that the forward PQ mechanism is to be considered different for the background absorption (which quenches for  $T < 125$  K) and for wall absorption (which quenches for  $T < 80$  K). The same observation is made for direct and inverse contrast wavelength domain.

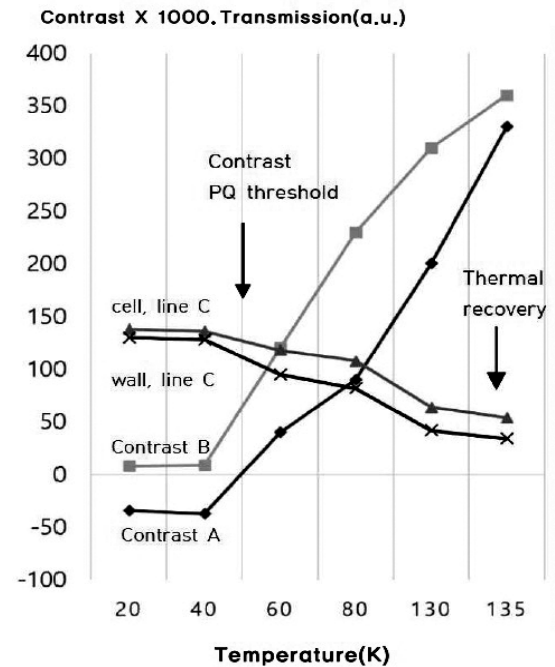


Fig. 8 Transmission and contrast vs PQ temperature

It could be valuably deduced that the walls preferentially contain a particular EL2 (let us denote it EL2w) which quenches at lower temperature than the other EL2 (EL2b) which is homogeneously distributed in the bulk of the material.

From typical values of the transmission before and after PQ the densities of EL2b and EL2w can be deduced from the equation (6). The resulting profiles are shown in Fig. 9(a) for measurements at wavelength of  $1 \mu\text{m}$  and in Fig. 9(b) for measurements in band gap region (inverse contrast). Both results are consistent and show an increased density of EL2w and a small reduction of EL2b in the region of the walls where there is a high density of dislocations. In Fig. 9(b) is also given the residual transmission profile which can be explained in terms of inverse contrast absorption sites.

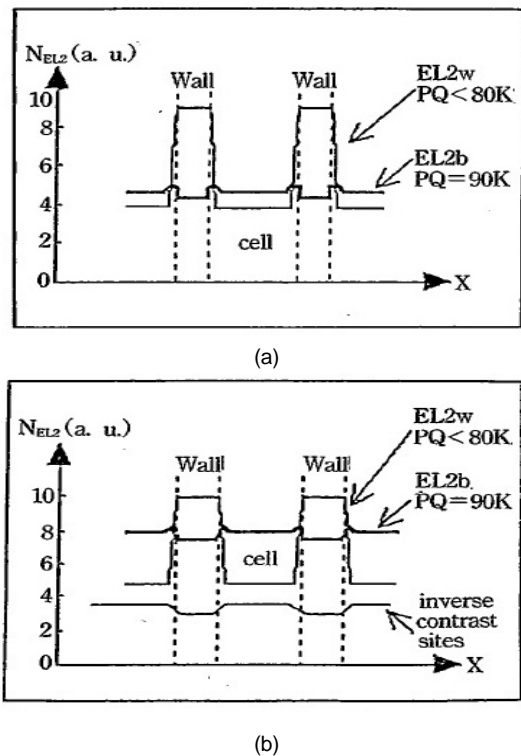


Fig. 9 Density profiles deduced from the logarithmic deviations in the transmission profiles: (a)  $1 \mu\text{m}$  region, (b) band edge region.

Another point to take into consideration is the behavior of the images in the range of the high absorption close to the gap. It was observed that this region is sensitive to PQ which gives rise to an inverted contrast images [1]. But further investigations showed that the inverted image still exists before quenching [2]. Many shallow traps were identified in this energy range which are related to EL2 [6]. The stability of this image with respect to PQ leads to the opinion that it belongs to an absorption mechanism independent of EL2 or to a coherence artefact of diffracted photons or also to an effect of local gradient in the refractive index [6].

## V. CONCLUSIONS

The behavior of images in the region close to the gap is quantitatively analysed by means of spectral imaging technique. It has shown that spectral images of contrast are able to reveal unexpected information on the EL2 PQ phenomenon in standard LEC semi-insulating GaAs. The EL2 centers behave with different PQ temperature threshold depending on the whether they are located in the walls or in the cells. The difference in the threshold temperatures for the EL2w and EL2b defects could be attribute to the contribution of a different electrical assistance due to a different species of impurities. Quantitative analysis results show an increased density of EL2w and a small reduction of EL2b in the region of the walls where there is a high density of dislocations.

## ACKNOWLEDGEMENTS

The author is pleased to acknowledge Professor J.P. Fillard (Montpellier II, France) for very valuable discussions and expert technical assistance.

## REFERENCES

- [1] M. S. Skolnick, L. J. Reed, and A. D. Pitt, "Photoinduced quenching of infrared absorption nonuniformities of large diameter GaAs crystals," *Applied Physics Letters*, vol. 44, no. 4, pp. 447-449, Feb. 1984.
- [2] S. J. Kang, "Contribution à l'étude du centre EL2 dans GaAs semi-insolant par photoextinction des images de transmission infra-rouge," (Contribution to the study of EL2 centre in semi-insulating GaAs by photoquenching of infrared transmission images), Ph. D. dissertation, USTL (Montpellier II), France, 1990.
- [3] S. J. Kang and C. H. Na, "Direct observation of wavelength dependent spectral response of CCD sensors," *Information: An International Interdisciplinary Journal*, vol.17, no.11(B), pp. 5831-5836, Nov. 2014.
- [4] P. Gall, J. P. Fillard, M. Castagné, J. L. Wayer and J. Bonnafé, "Microtomography observation of precipitated in semi-insulating GaAs materials," *Journal of Applied Physics*. vol.64, no.10, pp. 5161-6169, Nov. 1988.
- [5] P. Silverberg, P. Omling, and L. Samuelson, "Computer based mapping of concentration and occupation of EL2 in GaAs wafers," in *Proceedings of the 2<sup>nd</sup> International Symposium on Defect Recognition and Image Processing in III-V Compounds (DRIP II)*, Monterey: California, pp. 281-288, 1987.
- [6] S. J. Kang, "Infrared imaging and a new interpretation on the reverse contrast images in GaAs wafer," *Journal of the Korea Institute of Information and Communication Engineering*, vol. 20, no.11, pp. 2085-2092, Nov. 2016.



**강성준(Seong-Jun Kang)**

1990.3 (프) U.S.T.L(Montpellier II) 전자공학박사(Doctorat)  
1980.4-1994.2 한국전자통신연구원(ETRI) 책임연구원  
1994.3~ 현재 목포대학교 전자·정보통신공학과 교수  
※관심분야: IRT영상기술, 전자통신



**나철훈(Cheolhun Na)**

received the B.S., M.S. and Ph. D. degree from Electrical Engineering, Chonnam National University, Korea in 1985, 1987, and 1994, respectively. From 1995, he worked as a professor of Mokpo National University. His research interest is in the area of digital image processing, communication engineering, and medical image.